Desalination and Water Treatment
www.deswater.com

doi:10.5004/dwt.2017.21046

83 (2017) 98–110
July

Highly efficient removal of phosphate using a novel Fe-La binary (hydro) oxide as adsorbent: behavior and mechanism

Wei Zhang[a,b], Xiaowen Wang[c], Jing Chen[a], Gaosheng Zhang[a,*]

[a]*Key Laboratory of Coastal Zone Environmental Processes, Yantai Institute of Coastal Zone Research (YIC), Chinese Academy of Sciences (CAS), 17th Chunhui Road, Yantai, Shandong 264003, China, Tel. +86 05352109139, Fax +86 0535 2109139, email: zhangwei@yic.ac.cn (W. Zhang), jchen@yic.ac.cn (J. Chen), gszhang@yic.ac.cn (G.S. Zhang)*
[b]*State Key Laboratory of Urban Water Resource and Environment, School of Municipal and Environmental Engineering, Harbin Institute of Technology, Harbin 150090, China*
[c]*Yantai No.2 Middle School of Shandong Province, 57th Chuangxin Road, Yantai, Shandong 264003, China, email: missmarkwang@163.com (X.W. Wang)*

Received 30 December 2016; Accepted 17 June 2017

ABSTRACT

Phosphate has been proved to be one of the main elements causing eutrophication of water bodies. However, the elevated phosphate concentrations in the water bodies are often due to the excess discharge of wastewater containing phosphate. Therefore, treatment of elevated phosphate-containing wastewater is of vital importance to alleviate the situation. In this study, a novel Fe-La binary (hydro) oxide adsorbent was synthesized via a facile coprecipitation method for effective phosphate removal from wastewater. The adsorbent grains were formed of primary nanoparticles. Batch experiments were carried out to investigate adsorption kinetics and equilibrium. The adsorption was fast and well fitted by the pseudo-second-order equation, indicating that the adsorption process might be chemical sorption. The adsorption isotherms could be well described by Freundlich model and the maximal adsorption capacity reached 80.7 mg/g at pH 6.0 ± 0.1 and 67.4 mg/g at pH 9.0 ± 0.1, respectively, much higher than many reported adsorbents. The phosphate adsorption was pH dependent and weakly acidic condition was favorable for the adsorption. The phosphatead sorption might be mainly achieved via the replacement of surface hydroxyl groups at the solid surface and the formation of inner-sphere surface complexes. Moreover, the spent adsorbent could be effectively regenerated using dilute NaOH solution and used repeatedly. All these results suggest that the adsorbent maybe a promising alternative for phosphate removal.

Keywords: Fe-La binary (hydro)oxide; Phosphate; Adsorption; Removal

1. Introduction

As an indispensable macronutrient, phosphorus is very essential for biomass growth and the normal functioning of ecosystems [1,2]. In aqueous environment, phosphorus exists in the pentavalent form as orthophosphate, pyrophosphate, longer-chain polyphosphates, organic phosphate esters and phosphodiesters, and organic phosphonates, and these various phosphorus compounds could be hydrolyzed to orthophosphate, the only form of phosphorus that could be utilized by bacteria, algae, and plants [3]. However, excess discharge of phosphate into water body often causes eutrophication, and results in worsening of water quality [4,5]. It is thought that algae bloom or red tide will ensue once the concentration of phosphate in lakes or sea is over 0.03 mg/L [6]. To minimize these health risks, a maximum discharge limit of phosphorus of 0.5–1.0 mg/L set by the World Health Organization (WHO) has been adopted in many countries and regions [7]. Consequently, wastewater containing elevated phosphate must be treated to meet the limit before being discharged into natural surface water bodies.

*Corresponding author.

Various treatment technologies have been studied for the removal of phosphate from wastewater, such as chemical precipitation [8], adsorption [9], biological removal [10], reverse osmosis [11], membrane [11], ion exchange [12], and constructed wetlands [13]. Among these obtainable approaches, chemical precipitation and biological removal are normally not able to meet the stringent effluent standards and reverse osmosis is expensive, while the adsorption method proves to be more hopeful in term of flexibility and simplicity of design, ease of operation and high uptake capacity. Another attractive feature of this technique is that the nutrient-loaded filters can be used in agriculture as phosphate fertilizer and soil conditioner [14]. A variety of materials including natural and synthetic ones, have been used as adsorbents for phosphate removal in the literatures [15–21]. Iron is the second most abundant metal in the earth's crust and its (hydro) oxides are low-cost, environment-friendly. Because of strong affinity towards phosphorus species, Fe (hydro) oxides materials, including amorphous hydrous ferric oxide, poorly crystalline hydrous ferric oxide (ferrihydrite) [22], goethite and akaganeite [23,24], have been extensively studied for phosphate removal. Most recently, increasing efforts have been devoted to the synthesis of novel composite adsorbents containing iron oxides, including Fe-Mn [25], Fe-Al [26], Fe-Cu [27], Fe-Zr [28], Fe-Ti [29], Fe-Ag [30], Ca-Fe [31], etc. These omposites possess superior adsorption performance for phosphate than their individual components.

Lanthanum (La), a rare earth element, is considered to be non-toxic and environmental-benign. Lanthanum (hydro) oxides exhibit specific affinity towards phosphate even at trace levels [32,33]. Recently, phosphate removal using lanthanum (hydro) oxides has attracted growing attention [34,35]. To improve the cost-efficiency for phosphate removal, lanthanum (hydro)oxides have also been widely doped in metal oxides or loaded in porous materials to produce efficient composite adsorbents [7,36–42]. These composite adsorbents usually diminish the aggregation of nanoparticles, improving the phosphate removal efficiency. Moreover, the binding between lanthanum (hydro) oxides and other components may suppress the leakage of La ion in to water, which probably decreases biological incompatibilities.

In our previous study, a novel Fe-La binary (hydro)oxide was synthesized by a facile chemical precipitation method at ambient temperature and was found to have a strong affinity for arsenate [43]. Phosphorus and arsenic belong to the same element group (main group V). Therefore, phosphate and arsenate are very similar in molecular structure and chemical property. Previous results showed that the present phosphate competed strongly with arsenate for sorption sites on surface of the Fe-La binary (hydro)oxide [43], indicating that it also might be an excellent phosphate adsorbent. However, to date, no information is available on the phosphate removal by the Fe-La binary (hydro) oxide.

Thus, a novel Fe-La binary (hydro) oxide with a Fe/La molar ratio of 2:1 was synthesized and tested for phosphate removal in this study. The phosphate adsorption experiments including adsorption kinetics and adsorption isotherm were studied in detail. The influences of various experimental parameters, such as solution pH, ionic strength, and competitive anions on phosphate removal were examined. Furthermore, the removal mechanism of phosphate was investigated by both macroscopic and microscopic techniques.

2. Materials and methods

2.1. Materials

Anhydrous potassium dihydrogen orthophosphate (KH_2PO_4) are guaranteed grade and other reagents including $FeCl_3{\cdot}6H_2O$, $LaCl_3{\cdot}nH_2O$ and NaOH are analytical grade. Phosphate stock solutions were prepared with deionized water and KH_2PO_4. Phosphate working solutions were freshly prepared by diluting phosphate stock solutions with deionized water. The concentrations of phosphate species were always given as elemental phosphorus concentration in this study.

2.2. Adsorbent preparation

The Fe-La binary (hydro) oxide with a Fe/La molar ratio of 2:1 was prepared at room temperature (25°C), according to the following procedure: Ferric chloride ($FeCl_3{\cdot}6H_2O$, 0.02 mol) and lanthanum chloride ($LaCl_3{\cdot}nH_2O$, 0.01 mol) were dissolved in 500 mL of deionized water. Under vigorous stirring, sodium hydroxide solution (NaOH, 2 mol/L) was added drop wise to raise the solution pH to around 8.5. After addition, the formed suspension was continuously stirred for 1 h, aged at room temperature for 4 h and then washed several times with deionized water. The suspension was then filtrated and dried at 55°C for 24 h. The dried material was crushed and stored in a desiccator for use. The obtained powder adsorbent was named as Fe-La binary (hydro)oxide.

2.3. Adsorbent characterization

The morphology of the particles was characterized by a field scanning electron microscope (FESEM) coupled with energy dispersive X-rayspectroscopy (EDS) (Hitachi S-4800, Japan). X-ray diffraction (XRD) analysis was carried out on a D/Max-3A diffractometer (Rigaku Co., Japan) using Ni-filtered copper Ka_1 radiation. The specific surface area was measured via nitrogen adsorption using BET method with a Micromeritics ASAP 2000 surface area analyzer (Micromeritics Co., USA).

A zeta potential analyzer (Zetasizer 2000, Malvern, UK) was used to analyze the zeta potential of the Fe-La binary (hydro) oxide particles before and after phosphate adsorption. The content of the Fe-La binary (hydro) oxide in the solution was about 200 mg/L and phosphate concentration was 15 mg/L. $NaNO_3$ was used as background electrolyte to maintain an approximately constant ionic strength of 0.01 M. After mixing for 72 h to ensure the achievement of adsorption equilibrium, 5 mL of the suspension was transferred to a sample tube. Zeta potential of the suspension was then measured by electro kinetic analysis.

FTIR spectra were collected on a Nicolet IS10 FTIR spectrophotometer (Thermo scientific, USA) using a transmission model. Samples for FTIR determination were ground with spectral grade KBr in an agate mortar. IR spectra of

phosphate adsorbed onto the Fe-La binary (hydro) oxide were obtained from dry samples in KBr pellets corresponding to 5 mg of sample in approximately 200 mg of KBr. All IR measurements were carried out at room temperature.

X-ray photoelectron spectra (XPS) were collected on an ESCALab-220i-XL spectrometer with a monochromatic Al Ka X-ray source (1486.6 eV). C1s peaks were used as an inner standard calibration peak at 284.7 eV. For wide-scan spectra, an energy range of 0–1100 eV was used with pass energy 80 eV and step size 1 eV. The high-resolution scans were conducted according to the peak being examined with pass energy 40 eV and step size 0.05 eV. The XPS results were collected in binding energy forms and fitted using a nonlinear least-squares curve-fitting program (XPSPEAK41 Software).

2.4. Batch adsorption tests

2.4.1. Adsorption kinetics

The kinetics experiments were carried out at room temperature (25 ± 1°C). Predetermined amount of phosphate stock solution and $NaNO_3$were added in a 1000-mL glass vessel and then diluted to 500 mL with deionized water. The initial phosphate concentration was 5 mg/L. The ionic strength of the solutions was 0.01 M. After the solution pH was adjusted to 6.0 ± 0.1 by adding 0.1 M HNO_3 and/or NaOH, 0.1 g of Fe-La binary (hydro) oxide was added to obtain a 0.2 g/L suspension. The suspension was mixed with a magnetic stirrer at an agitation speed of 170 rpm, and the pH was maintained at 6.0 ± 0.1 throughout the experiment by addition of dilute HNO_3 and/or NaOH solution. Approximately 5 mL samples were taken from the glass vessel at predetermined times. The samples were immediately filtered through a 0.45-μm membrane filter and residual phosphate concentrations in filtrates were determined. The adsorbent powders were taken out for further characterization.

2.4.2. Effect of solution pH and ionic strength

The influences of solution pH and ionic strength on the phosphate adsorption were investigated by adding 10 mg of Fe-La binary (hydro)oxide into 100-mL plastic vessels, containing 50 mL of phosphate solution. Initial phosphate concentration was 15 mg/L and the sorbent dosage was 0.2 g/L. The ionic strength of the solutions varied from 0.001 to 0.1 M by adding different amounts of $NaNO_3$. The pH of the solutions was adjusted every 4 h with dilute HNO_3 or/and NaOH solution to designated values in the range 3–11 during the shaking process. The equilibrium pH was measured and the supernatant was filtered through a 0.45-μm membrane for phosphate measurement after the solutions were mixed for 24 h. In addition, to evaluate the leaching of Fe and La from the adsorbent at different pH, the Fe and La concentrations in the supernatant solutions were also measured by ICP-OES.

2.4.3. Adsorption isotherms

The phosphate adsorption isotherm was determined using batch tests at respective pH, 6.0 ± 0.1 and 9.0 ± 0.1. The pH of suspensions was adjusted with 0.1 M HNO_3 and/or NaOH during the experiment. Initial phosphate concentration varied from 2 mg/L to 60 mg/L. In each test, 10 mg of Fe-La binary (hydro) oxide was loaded in a 100-mL plastic vessel containing 50 mL phosphate solution of predetermined concentration. Ionic strength of the solution was adjusted to 0.01 M with $NaNO_3$. The vessels were shaken on an orbit shaker at 170 rpm for 24 h at 25 ± 1°C. Then, all samples were filtered by a 0.45-μm membrane filter and analyzed for phosphate. The quantity of adsorbed phosphate was calculated by the difference of the initial and residual amounts of phosphate in solution divided by the weight of the adsorbent.

2.4.4. Effect of coexisting anions

The effect of common coexisting ions in wastewater such as Cl^-, CO_3^{2-}, SO_4^{2-} and SiO_3^{2-} on the phosphate adsorption was investigated by adding NaCl, Na_2CO_3, Na_2SO_4 and Na_2SiO_3 to 10 mg/L (about 0.0003 M) of phosphate solution, respectively. The anion concentrations ranged from 0.0001 to 0.01 M. The solution pH was adjusted to 6.0 ± 0.1 with dilute HNO_3 or/and NaOH solution. 10 mg of Fe-La binary (hydro) oxide was added in each of the vessel and the solutions were mixed at 170 rpm for 24 h at 25 ± 1°C. After filtration by a 0.45 μm membrane filter, the residual concentration of phosphate in the samples was analyzed.

2.4.5. Regeneration and reusability of the Fe-La binary (hydro) oxide

The regeneration and recycle of the spent adsorbent were studied. For the adsorption test, 400 mg of the Fe-La binary (hydro) oxide was introduced into 2 L phosphate solution of 10 mg/L. The solution was stirred continuously for 24 h at 170 rpm and 25 ± 1°C. The pH of the solution was maintained at 6.0 ± 0.1 during adsorption process. Then the spent adsorbent was separated by filtration and was used for desorption test after drying at 55°C for 2 h. The residual phosphate concentration n the filtrates was measured using the ICP-OES. For the desorption tests, the spent adsorbent was added into 100 mL NaOH solution of 0.5 mol/L. The mixture was stirred for 4 h and then separated from the NaOH solution. After washing and drying, the adsorbent was to be used in the next adsorption-desorption cycle. The regeneration/recycle experiment was conducted for four cycles to evaluate the re usability of the adsorbent.

2.5. Analytical methods

Phosphate concentration was determined by an ICP-OES (Optima 7100 DV, Perkin Elmer Co. USA). Prior to analysis, the aqueous samples were acidified with concentrated HCl in an amount of 1% and stored in acid-washed glass vessels. All samples were analyzed within 24 h after collection.

3. Results and discussion

3.1. Characterization of the Fe-La binary (hydro) oxide

The morphology and surface element distribution of Fe-La binary (hydro) oxide were examined by FESEM and

EDS. The SEM image (Fig. 1A) shows that it was aggregates formed compactly by nano particles with a size range of 20–40 nm and nanoflakes with a size range of 50–150 nm, which resulted in an irregular and rough surface and a porous structure. The EDS analysis (Fig. 1B) revealed that Fe and La were evenly distributed on the surface and the Fe/La molar ratio on the surface was about 2.18, a little higher than that of bulk, which was in the range of 1.93–2.07.

The powder X-ray diffraction pattern of the Fe-La binary (hydro) oxide is illustrated in Fig. S1 (supplementary materials). It showed some sharp and symmetric reflections for (100), (101), (201) and (300) planes, which were similar to the XRD pattern of $La(OH)_3$ (JCPDS 36-1481) [44]. In addition, no other peaks were detected, indicating that the Fe (hydro) oxide component was amorphous.

The N_2 adsorption and desorption isotherms of the Fe-La binary (hydro) oxide are shown in Fig. S2A. The adsorption and desorption isotherms of Fe-La binary (hydro) oxide were type IV according to the IUPAC classification [45]. The Fe-La binary (hydro) oxide material was possibly mesoporous, as it demonstrated a hysteresis loop for the desorption isotherm [45]. The adsorption isotherms of Fe-La binary (hydro) oxide did not present a plateau at high P/P_o values, indicating that these pores might be produced by aggregation of random layer structure-like particles. The data of specific surface area, average pore diameter, and average pore volume of Fe-La binary (hydro) oxide are listed in Table S1. It could be seen that the Fe-La binary (hydro) oxide had a high specific surface area of 120.1 m^2/g with a pore volume of 0.168 cm^3/g. The pore size distribution of this adsorbent is shown in Fig. S2B. The adsorbent presented a wide pore size range from 30 to below 3 nm.

3.2. Batch adsorption experiments

3.2.1. Kinetics of phosphate adsorption by the Fe-La binary (hydro) oxide

Adsorption rate is an important factor in terms of evaluating the adsorption efficiency and mechanism of the sorbent. Therefore, the kinetics of phosphate adsorption on Fe-La binary (hydro) oxide was investigated in this study and the kinetics data is shown in Fig. 2A. The adsorption increases fast in the initial period, and over 95% of the equilibrium adsorption capacity is achieved within the beginning 1 h. Afterwards, the adsorption process slows down and about 12 h are required to reach the adsorption equilibrium. Therefore, all other batch experiments are carried for 24 h to ensure complete adsorption.

In order to evaluate the kinetic mechanism that controls the adsorption process, kinetic data analysis for phosphate adsorption was studied with the pseudo-first-order model [46], the pseudo-second-order model [47], the elovich model [48] and the intraparticle diffusion model [49]. The mathematical representations of the models are given in:

$$\frac{dq_t}{dt} = k_1(q_e - q_t) \quad (1)$$

$$\frac{dq_t}{dt} = k_2(q_e - q_t)^2 \quad (2)$$

$$q_t = A + k_3 \ln t \quad (3)$$

$$q_t = k_p t^{0.5} \quad (4)$$

where q_e and q_t are the adsorption capacities (mg/g) of the adsorbent at equilibrium and at any time t (h), respectively; k_1(h^{-1}), k_2 (g/mg·h), k_3 and k_p are the related adsorption rate constants; A is constant; and C is a constant gained from the intercept of plot of q_t against $t^{0.5}$.

The rate constants obtained from the pseudo-first-order, the pseudo-second-order and the Elovich models are summarized in Table 1. It could be found that the experimental data fitted the pseudo-second-order model (the higher correlation coefficient values) better than the pseudo-first-order and the elovich models, and the chemical adsorption was the potential rate controlling step in the phosphate adsorption. Since the pseudo-second-order kinetic model is based on the assumption that the rate-limiting step may be chemisorption involving valence forces through sharing or exchange of electrons between sorbent and sorbate [47].

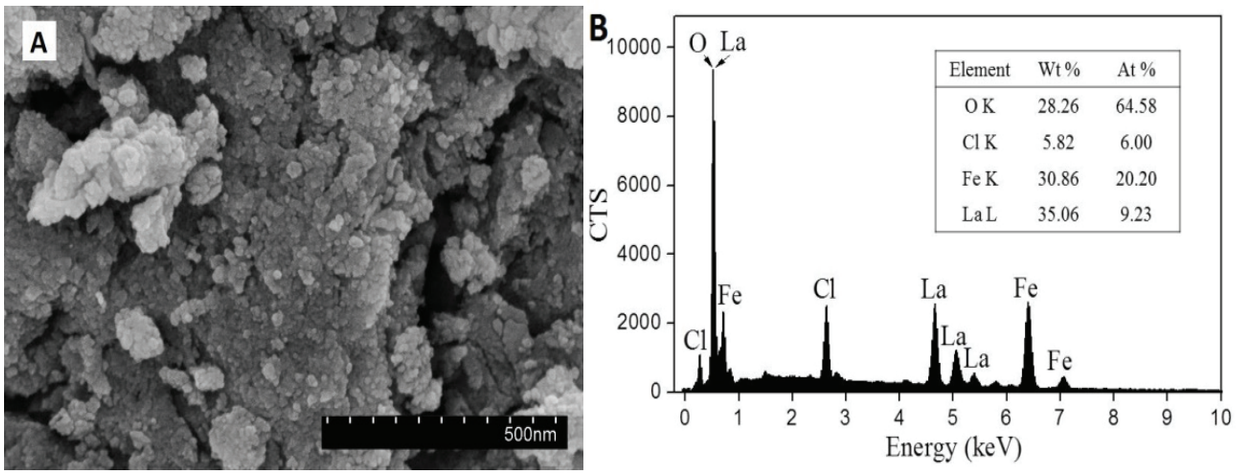

Fig. 1. SEM micrograph (×100000) (A) and EDS surface analysis (B) of the Fe-La binary(hydro) oxide.

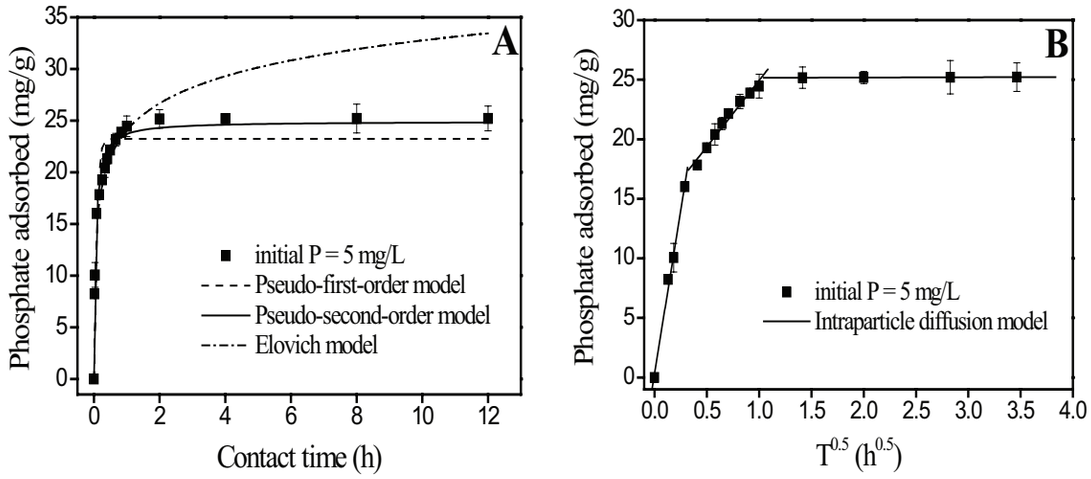

Fig. 2. Kinetics of phosphate removal by the Fe-La binary (hydro)oxide. (A) Phosphate fitted with pseudo-first-order model, pseudo-second-order model and elovich model, (B) Phosphate fitted with intraparticle diffusion model. Initial phosphate concentrations = 5 mg/L, adsorbent dose = 200 mg/L, pH = 6.0 ± 0.1, agitation speed = 170 rpm, T = 25 ± 1°C.

Table 1
Adsorption rate constant obtained from pseudo-first-order model, pseudo-second-order model and elovich model

Adsorbent species	Pseudo-first-order model			Pseudo-second-order model			Elovich model	
	k_1 (h^{-1})	q_e (mg/g)	R^2	k_2 (g/mg·h)	q_e (mg/g)	R^2	k_3	R^2
Fe-La	13.42	23.24	0.917	0.78	24.92	0.983	3.786	0.972

The reaction kinetics is well fitted to the pseudo-second order rate model, but this model is limited in accuracy by considering adsorption as a single, one-step binding process [28]. However, the intraparticle diffusion model may provide a more comprehensive view of adsorption as a series of distinct steps [49]. Therefore, it was also applied to fit the experimental data. From Fig. 2B, it can be clearly found that the whole plot includes three linear sections and this multi-linearity indicates further the complexity of the adsorption process. The first linear step was a fast stage. Transferring of phosphate anions from bulk phase to particle surface was rapid since the adsorption was conducted in a well-agitated tank. For well-agitated system, film diffusion resistance will be quite small and pore diffusion will be rate controlling. The second linear portion was a moderate sorption process, governing by the intraparticle diffusion in the pore structure. The third linear section was a very slow adsorption stage, attributing to the steric hindrance from the adsorbed molecules [28].

3.2.2. Effect of pH and ionic strength

The effects of pH and ionic strength on the adsorption of phosphate were assessed and the results are demonstrated in Fig. 3A. It could be seen that the removal percentage of phosphate by the Fe-La binary (hydro) oxide was high under acidic conditions, while decreased with increasing solution pH under alkaline conditions. Similar results were observed for phosphate adsorption on Fe-Cu binary oxides [27] and nanocomposite Ws-N-La [37]. Adsorption of strong acid anions by metal oxides and hydroxides typically decreases with increasing pH [50]. The species distribution of phosphate is known to vary with pH values. In water, phosphate can exist as H_3PO_4, $H_2PO_4^-$, HPO_4^{2-} or PO_4^{3-}, depending on the pH (pK_1 = 2.15, pK_2 = 7.20, and pK_3 = 12.33) [17,50]. At pH 6.0, $H_2PO_4^-$ is dominant, accounting for over 80% of total phosphate species, while HPO_4^{2-} is the main phosphate species at pH 10.6. Low pH is favorable for the protonation of the sorbent surface. Increased protonation is thought to increase the positively charged sites, enlarging the attraction force existing between the sorbent surface and phosphate anions. Therefore, high adsorption capacity of phosphate on the sorbent was detected in the low pH region. With the increase in solution pH, the negatively charged sites gradually increase and enhance the repulsion effect, which in turn reduces the amount of adsorption. As a result, phosphate adsorption by the sorbent dropped gradually.

No significant change was found on phosphate adsorption as the ionic strength increased from 0.001 to 0.1 M. It is well known that the adsorption of phosphate would decrease with an increase in ionic strength if phosphate formed outer-sphere surface complexes; while the adsorption of phosphate would either not change or increase with increasing ionic strength if phosphate formed inner-sphere complexes [51]. Thus, the results in this study demonstrated that phosphate anions might be specifically adsorbed on the

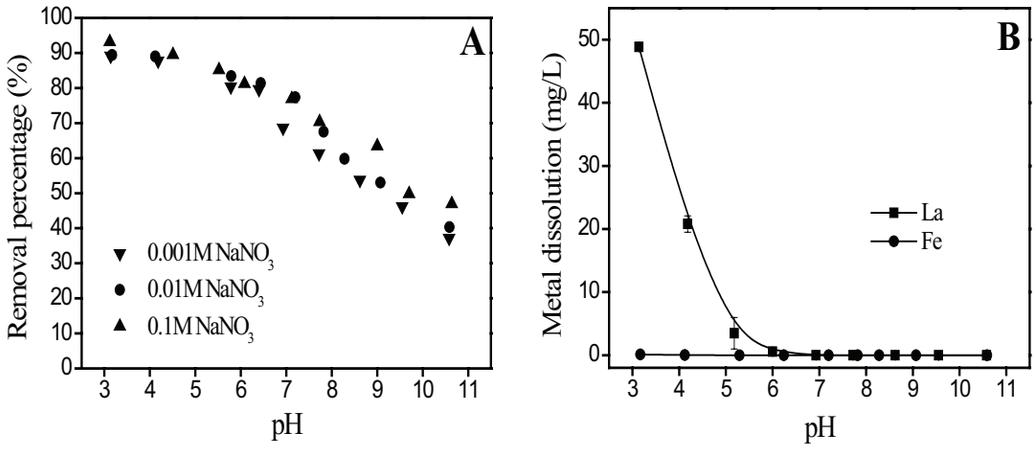

Fig. 3. (A) Removal percentage of phosphate by the Fe-La binary (hydro) oxide and (B) the leaching of La^{3+} and Fe^{3+} ion. Initial phosphate concentration = 15 mg/L, adsorbent dose = 200 mg/L, agitation speed = 170 rpm, T = 25 ± 1°C.

Fe-La binary (hydro) oxide via forming inner-sphere surface complexes.

Additionally, the leaching of Fe and La from the adsorbent at different pHs was evaluated and shown in Fig. 3B. The leaching of Fe^{3+} ion from Fe-La binary (hydro) oxide was negligible in the tested pH range. However, obvious leaching of La^{3+} ion occurred under acidic conditions. It decreased markedly with increasing solution pH and became negligible at pH > 6. Similar results were observed for removal of phosphate by Fe-Mg-La tri-metal composite adsorbent and lanthanum hydroxide materials [7,35]. In the low pH region, the leached La^{3+} ion may easily react with phosphate to form insoluble lanthanum phosphate (solubility product of lanthanum phosphate pK = 26.15 [52]). Therefore, the phosphate removal might be accomplished through both adsorption and forming precipitation of lanthanum phosphate under acidic conditions. Nevertheless, the pH of natural water is generally higher than 6.5. At this point, the leaching of La^{3+} ion is very little and the hydroxide precipitation formed is negligible. Thus, the phosphate uptake might be attributed only to adsorption under neutral and alkaline conditions.

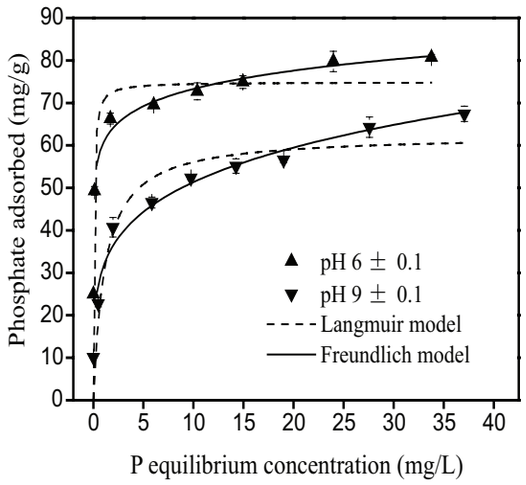

Fig. 4. Isotherms for phosphate adsorption by the Fe-La binary (hydro) oxide at pH 6.0 ±0.1 and pH 9.0 ±0.1. Adsorbent dose = 200 mg/L, agitation speed = 170 rpm, T = 25 ± 1°C.

3.2.3. Adsorption capacity of the Fe-La binary (hydro) oxide

Batch adsorption experiments were carried out to determine the maximum adsorption capacity of phosphate on the Fe-La binary (hydro) oxide. Fig. 4 shows the plots of the phosphate adsorbed by the adsorbent against the phosphate equilibrium concentration in the solution at pH 6.0 ± 0.1 and pH 9.0 ± 0.1, respectively. Both Langmuir and Freundlich models [53,54] were employed to describe the adsorption isotherms obtained in the figure. The two equations can be expressed as follows:

$$q_e = \frac{q_{\max} K_L C_e}{1 + K_L C_e} \tag{5}$$

$$q_e = K_F C_e^n \tag{6}$$

where q_e and q_{max} represent the amount of equilibrium adsorption capacity and the maximum adsorption capacity (mg/g), respectively; K_L (L/mg) is the Langmuir coefficient; C_e is the equilibrium solution concentration (mg/L); K_F is roughly an indicator of the adsorption capacity and n is an empirical parameter; n is the heterogeneity factor, which has a lower value for more heterogeneous surfaces.

The adsorption constants obtained from the isotherms were listed in Table 2. Evidently, the Fe-La binary (hydro) oxide has a higher adsorption capacity at a lower pH value, which is consistent with the result of solution pH effect on adsorption. As shown in Table 2, the equilibrium data for the adsorption of phosphate onto the Fe-La binary (hydro) oxide could be better described by the Freundlich isotherm model than Langmuir model at the two pH levels. It is not surprising that the Langmuir equation failed in describing the adsorption behavior of phosphate because this model assumes that adsorption occurs on a homogeneous surface. The presence of La (hydro) oxide in the adsorbent may lead

to a more heterogeneous surface of solid. The Freundlich equation describes adsorption where the adsorbent has a heterogeneous surface with adsorption sites that have different energies of adsorption. Direct graphic maximal removal capacity (corresponding to the isotherm plateau) gives a maximal capacity of 80.7 mg/g at pH 6.0 ± 0.1 and 67.4 mg/g at pH 9.0 ± 0.1, respectively.

Table 3 shows the comparison results of the maximum adsorption capacities of various adsorbents for phosphate. It was found that the prepared Fe-La binary (hydro) oxide outperformed many other adsorbents. Especially, it should be noted that the high adsorption capacity of the Fe-La binary (hydro) oxide was achieved at a low equilibrium concentration (0.5 mg/L). All these results suggest that the adsorbent maybe used as a promising adsorbent for phosphate removal from aqueous media.

3.2.4. Effect of coexisting anions

As well known, adsorption selectivity influences significantly removal effectiveness. Some researchers applied highly selective adsorbents to remove heavy metals from aqueous systems [57–59]. Coexisting ions such as silicate, chloride, sulfate, and carbonate are generally present in the wastewater, and might interfere in the uptake of phosphate through competitive adsorption. Herein, the effects of these coexisting anions at three concentration levels (0.0001, 0.001 and 0.01 M) on the phosphate adsorption were examined at initial pH of 6.0 ± 0.1 and the results were shown in Fig. 5.

It could be seen that for chloride and sulfate, no observable decrease in phosphate adsorption was detected when their concentrations increased from 0.0001 to 0.01 M. Only a slight decrease was observed with increasing bicarbonate concentration. Obviously, the presence of these three anions has no significant influence on the phosphate adsorption. However, the coexisting silicate suppressed the phosphate adsorption notably. For an example, the phosphate adsorption rate reduced to 54% when the concentration of silicate increased from 0 to 0.01 M. Both silicon and phosphorus are located in the adjacent position in the periodic table of the elements, and the molecular structure of the silicate ion is very similar to that of the phosphate ion. The present silicate ions may strongly compete with phosphate ions

Table 2
Langmuir and Freundlich isotherm parameters for phosphate adsorption onto the Fe-La binary (hydro) oxide under different pH

pH	Langmuir model			Freundlich model		
	q_{max} (mg/g)	K_L (L/mg)	R^2	K_F (mg/g)	n	R^2
6	74.89	16.05	0.650	60.60	0.08	0.976
9	62.43	0.88	0.904	31.51	0.21	0.962

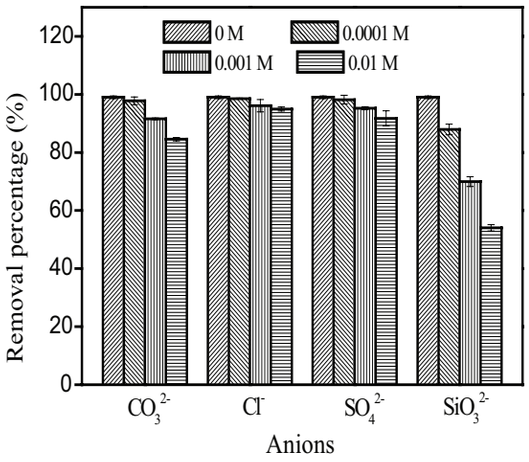

Fig. 5. Effect of coexisting anions on the phosphate removal performance with initial phosphate concentration at 10 mg/L. Adsorbent dose = 200 mg/L, pH 6.0 ± 0.1, agitation speed = 170 rpm, T = 25 ± 1°C.

Table 3
Comparison of maximum phosphate adsorption capacities for different adsorbents[a]

Sorbent material	Conc. range (mg/L)	Max. P adsorption capacity (mg/g)	Reference
Fe-La binary (hydro)oxide	0–35	80.7 (pH 6.0)	Present study
Fe-La binary (hydro)oxide	0–37	67.4 (pH 9.0)	Present study
Iron oxide tailings	0–131	8.2 (pH 6.6–6.8)	[55]
Al oxide hydroxide	0–9	35 (pH 6.0–7.0)	[6]
TEPA-Fe_3O_4- NMPs-1.0	32–650	102 (pH 3.0)	[17]
LDH 6c	0–200	300 (pH 6.5–7.0)	[20]
Mesoporous ZrO_2	0–275	29.7 (pH 6.7–6.9)	[56]
Fe-Cu binary oxide	0–25	35.2 (pH 7.0)	[27
Fe-Mn binary oxide	0–35	36 (pH 5.6)	[25]
Fe-Zr binary oxide	2–40	33.4 (pH 5.5)	[28]
La-doped vesuvianite	0–4	6.7 (pH 7.1)	[41]
La-modified bentonite	0–65	14 (pH 6.0)	[38]
La-doped mesoporous hollow silica spheres	0–50	47.9 (pH 5.0)	[39]

[a]pH is shown in parentheses.

for the binding sites on the adsorbent. Thus, phosphate adsorption is repressed and the phosphate adsorption rate reduces significantly.

3.2.5. Regeneration and reusability of the Fe-La binary (hydro) oxide

The regeneration and reusability of spent adsorbent are crucially important and directly influence the practicability of the adsorbent. Four successive adsorption-regeneration cycles were therefore carried out and the results are demonstrated in Fig. 6. The value of cycle 0 was the adsorption capacity of the fresh Fe-La binary (hydro) oxide. The phosphate adsorption capacity of the Fe-La binary (hydro) oxide slowly decreased with an increase in regeneration cycle. However, this reduction was not so remarkable and the adsorbent still retained more than 80% of its original phosphate adsorption capacity after 4 times regeneration, indicating that the phosphate-loaded adsorbent can be effectively desorbed and regenerated via 0.5 M NaOH treatment. Interestingly, the specific regeneration parameters differ greatly, due to the diverse adsorbents. Zhang et al. used 0.1 M NaOH to regenerate the phosphate-loaded Fe-Mn sorbent at room temperature [25]. Lu et al. also employed 0.1 M NaOH solution to treat the spent Fe-Ti sorbent at 20°C [29]. Yu et al. applied 0.5 M NaOH to desorb the spent Fe-Mg-La composite [7]. However, Zhang et al. found that a higher NaOH concentration of 2.5 M was necessary to regenerate effectively the spent composite Ws-N-La at 60°C [37]. Obviously, the Fe-containing composites were more easily to regenerate than the pure La-modified composite.

3.3. Analysis of the Fe-La binary (hydro) oxide before and after reaction with phosphate

3.3.1. Zeta potential study

Fig. 7 shows the zeta potentials of the Fe-La binary (hydro) oxide before and after phosphate adsorption. The isoelectric point (IEP) of the fresh Fe-La binary (hydro) oxide is found to be about pH 7.8, while the IEP of the phosphate-loaded sorbent is 7.1. The specific adsorption of anions makes the surface of oxides more negatively charged, which results in a shift of the IEP of adsorbent to a lower pH value [60]. The IEP of metal oxides is determined by protonation and deprotonation of surface hydroxyl groups. The formation of outer-sphere surface complexes cannot shift the IEP because there is no chemical reaction between the adsorbate and adsorbent surface [61]. Clearly, the phosphate removal is due to specific adsorption (chemical adsorption) rather than purely electrostatic interaction,in which inner-sphere surface complexes are formed.

3.3.2. Analysis of XPS

XPS spectra of Fe-La binary (hydro) oxide before and after reaction with phosphate were tested to verify the presence of phosphate and determine the oxidation state of adsorbed phosphate. Fig. 8A shows that the P2p core level peak had appeared after reaction with phosphate, which clearly indicated the presence of phosphate on the surface of Fe-La binary (hydro) oxide. Fig. 8B exhibits the P2p core level of Fe-La binary (hydro) oxide after the adsorption of phosphate. The P2p binding energy for the adsorbent was 133.1 eV, which suggested that the phosphorus onto the surface of the adsorbent existed in a pentavalent-oxidation state (P^{5+}) [62]. In other words, the oxidation state of phosphorus did not change during the reaction processes. Additionally, the XPS spectrum of P2p revealed the derivation of three peaks at 132.4, 133.2, and 134.3 eV, which correspond to the binding energies of PO_4^{3-}, HPO_4^{2-}, and $H_2PO_4^-$, respectively [62–65]. According to the area of three peaks, the phosphorus atomic ratio of PO_4^{3-}, HPO_4^{2-}, and $H_2PO_4^-$was calculated to be 24:69:7, which implied that the main phosphoric type presented on to the surface of Fe-La binary (hydro) oxide was HPO_4^{2-}. Furthermore, O1s narrow scans of the Fe-La binary (hydro) oxide before and after phosphate adsorption were collected and shown in Fig. 8C–D.The O1s peak could

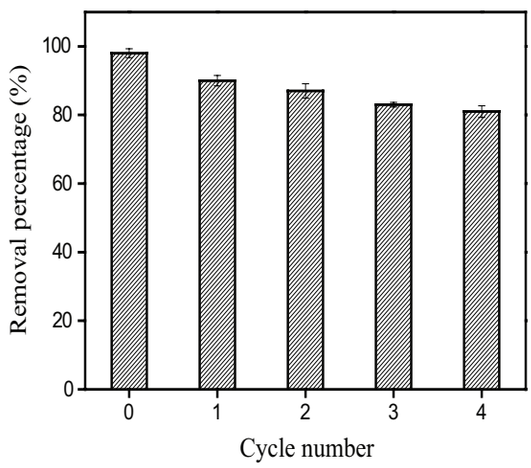

Fig. 6. Removal percentage of phosphate by the Fe-La binary (hydro) oxide in four successive adsorption-desorption cycles. Initial phosphate concentration = 10 mg/L, adsorbent dose = 200 mg/L, pH 6.0 ± 0.1, agitation speed = 170 rpm, T = 25 ± 1°C.

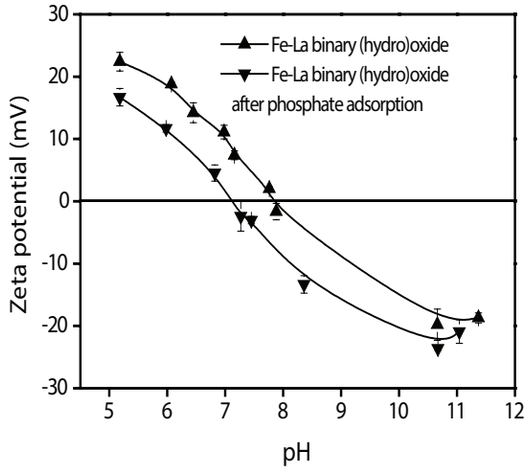

Fig. 7. Zeta potential of the Fe-La binary (hydro) oxide before and after phosphate adsorption at initial phosphate concentration = 15 mg/L. Adsorbent dose = 200 mg/L, ionic strength = 0.01 M $NaNO_3$, equilibrium time = 72 h.

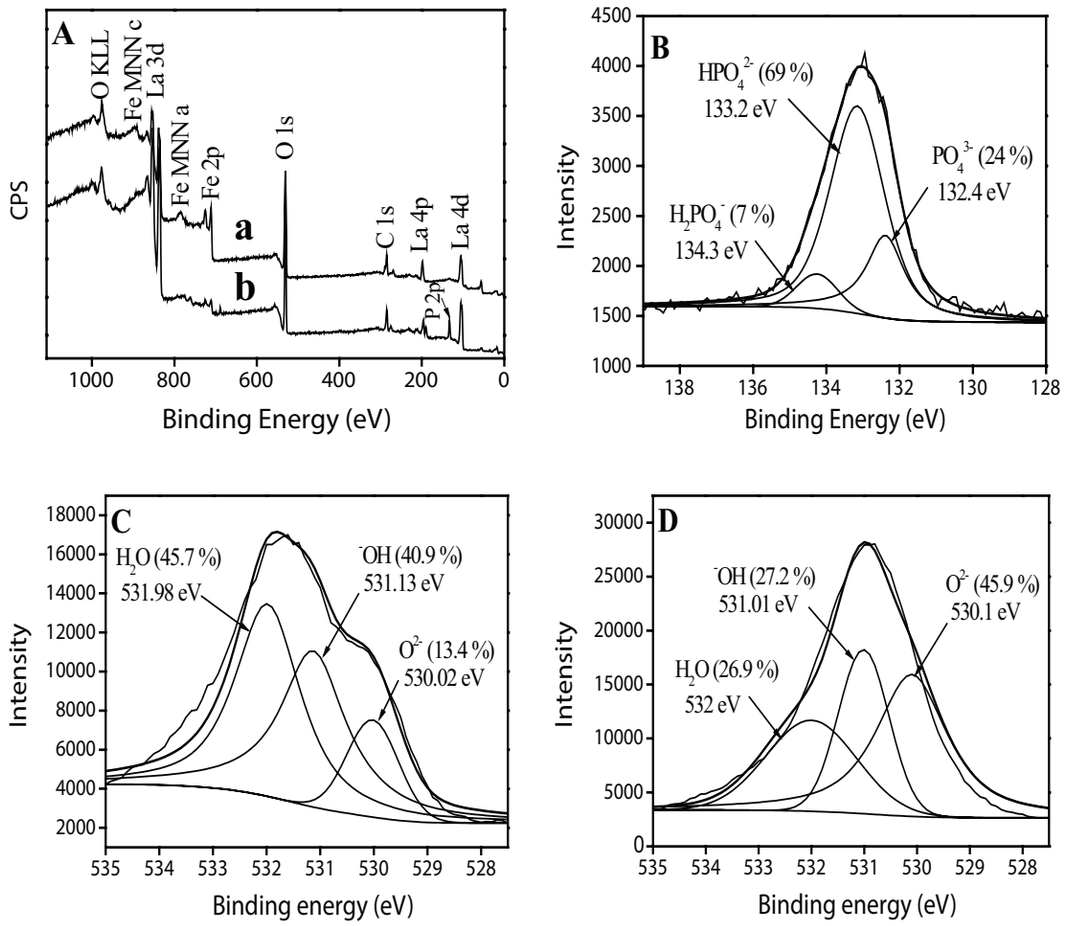

Fig. 8. XPS spectra of the Fe-La binary (hydro) oxide (a), after reaction with phosphate (b) (A); P2p core level of the adsorbent after reaction with phosphate (B); O1s spectra of the adsorbent (C) and O 1s spectra after phosphate adsorption (D).

be best fitted with three overlapped O1s peaks of oxide oxygen (O^{2-}), hydroxyl group (^{-}OH) and adsorbed water (H_2O) [7,64]. The spectra were fitted using a nonlinear least-square curve fitting program (XPSPEAK41 Software) and the fitting parameters can be found in Fig. 8C–D and SI Table 2. Fig. 8C demonstrates that the ^{-}OH percentage was about 40.9 % for the origin Fe-La adsorbent, while Fig. 8D shows that the ^{-}OH percentage largely dropped to about 27.2% after the phosphate adsorption. Meanwhile, the O^{2-} percentage signally increased after the phosphate adsorption, indicating that hydroxyl groups existed on the surface of the Fe-La binary (hydro) oxide and the ^{-}OH was partially replaced by phosphate and subsequently inner-sphere surface complexes were formed.

3.3.3. FTIR spectra

FTIR spectra of the Fe-La binary (hydro) oxide before and after reaction with phosphate were collected and are shown in Fig. 9. For the Fe-La binary (hydro) oxide sample, the bands at 3600–3200 cm^{-1} were assigned to the vibration of O-H stretching. The band at 1638 cm^{-1} could be ascribed to the deformation vibration of water molecules [7,23,25]. These indicated the presence of physisorbed water on the oxide. The peak at 1382 cm^{-1} was attributed to the vibration of adsorbed CO_3^{2-}, since the experiments was conducted in atmosphere [27]. The bands observed at 1483 cm^{-1} and 658 cm^{-1} were the characteristics of the lanthanum (hydro) oxide [40,43]. After phosphate sorption, the FTIR spectrum demonstrated obvious changed. It was found that the intensity of the peaks at 1483 cm^{-1} and 658 cm^{-1} was significantly weakened, meanwhile a new peak at 1057 cm^{-1} appeared, which was broad and intensive and could be assigned to the asymmetry vibration of P-O bond [25,66], indicating that the surface hydroxyl groups were replaced by the adsorbed phosphate and the phosphate was mainly bound as a surface complex.

3.4. Phosphate removal mechanism

From the results of the ionic strength effects experiment and the analyses of zeta potential along with XPS spectra, FTIR spectra, it can be reasonably concluded that phosphate is specifically adsorbed by the Fe-La binary (hydro) oxide through formation inner-sphere complex and the hydroxyl groups play a key role. Based on a direct in situ determina-

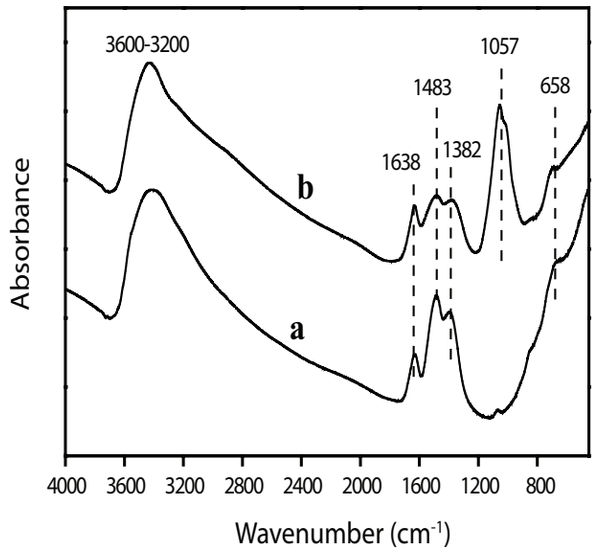

Fig. 9. FTIR spectra of the Fe-La binary (hydro) oxide (a), after reaction with phosphate (b).

tion of phosphate speciation using X-ray absorption spectroscopy, phosphate could form inner-sphere complexes on the surface of metal hydroxides, including the monodentate mononuclear and bidentate binuclear complexes [50]. The surface of the Fe-La binary (hydro) oxide was easily protonated and positively-charged at pH 6.0 [Eq. (7)], due to possessing a high pH_{PZC} (about 7.8). Thus, the phosphate removal process could be described as follows. Phosphate was firstly transported to the protonated surface by convection or diffusion from bulk solution. Then the phosphate was adsorbed through the replacement of surface hydroxyl groups and formation of monodentate mononuclear and bidentate binuclear inner-sphere surface complexes [Eqs. (8) and (9)].

$$S-OH+H^{+} \Longleftrightarrow S-OH_2^{+} \tag{7}$$

$$S-OH_2^{+}+H_2PO_4^{-} \Longleftrightarrow S-OPO_3H_2+H_2O$$

monodentae mononuclear (8)

$$2S-OH_2^{+}+H_2PO_4^{-} \Longleftrightarrow S_2O_2PO_2H+2H_2O+H^{+}$$

bidentate binuclear (9)

Fig. 10 demonstrates the reasonable major adsorption mechanism of phosphate on the Fe-La binary (hydro) oxide.

4. Conclusions

In this study, the preparation of the Fe-La binary (hydro) oxide was a simple and environment-friendly coprecipitation method. This adsorbent, with a high specific surface area (120.1 m^2/g), was formed by nanoparticles and nanoflakes. The pseudo-second-order equation describes the kinetic data well. The adsorbent had a high removal capacity toward phosphate. Maximal adsorption capacities were 80.7 mg/g at pH 6.0 ± 0.1 and 67.4 mg/g at pH 9.0 ± 0.1, respectively. The Fe-La binary (hydro) oxide was able to adsorb phosphate in the presence of competing anions and across a wide pH range. Among the coexisting anions, silicate was the greatest competitor with phosphate for adsorptive sites on the surface of oxide. Phosphate was adsorbed through the replacement of surface hydroxyl groups and formed inner-sphere surface complexes at the water/Fe-La binary (hydro) oxide interface.

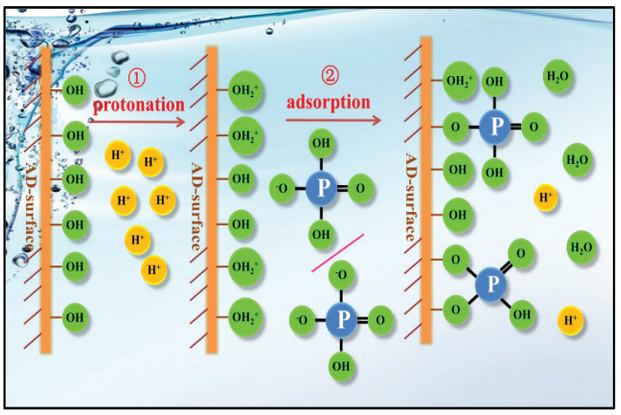

Fig. 10. Schematic diagram of the phosphate adsorption mechanism.

Acknowledgements

The authors acknowledge financial support by National Natural Science Foundation of China (Grant No. 51478457) andthe open Fund of the Jiangsu Key Laboratory for Environment Functional Materials (No. SJHG1312).

References

[1] P. Wilfert, P. Suresh Kumar, L. Korving, G.J. Witkamp, M.C. Van Loosdrecht, The relevance of phosphorus and iron chemistry to the recovery of phosphorus from wastewater: a review, Environ. Sci. Technol., 49 (2015) 9400–9414.
[2] C. Barca, C. Gérente, D. Meyer, F. Chazarenc, Y. Andrès, Phosphate removal from synthetic and real wastewater using steel slags produced in Europe, Water Res., 46 (2012) 2376–2384.
[3] D.L. Correll, The role of phosphorus in the eutrophication of receiving waters: A review, J. Environ. Qual., 27 (1998) 261–266.
[4] A.C.C. Rotzetter, C.R. Kellenberger, C.M. Schumacher, C. Mora, R.N. Grass, M. Loepfe, N.A. Luechinger, W.J. Stark, Combining phosphate and bacteria removal on chemically active filter membranes allows prolonged storage of drinking water, Adv. Mater., 25 (2013) 6057–6063.
[5] X. Xu, B.Y. Gao, W.Y. Wang, Q.Y. Yue, Y. Wang, S.Q. Ni, Adsorption of phosphate from aqueous solutions onto modified wheat residue: characteristics, kinetic and column studies, Colloids Surf., B 70 (2009) 46–52.
[6] S. Tanada, M. Kabayama, N. Kawasaki, T. Sakiyama, T. Nakamura, M. Araki, T. Tamura, Removal of phosphate by aluminum oxide hydroxide, J. Colloid Interface Sci., 257 (2003) 135–140.
[7] Y. Yu, J.P. Chen, Key factors for optimum performance in phosphate removal from contaminated water by a Fe-Mg-La tri-metal composite sorbent, J. Colloid Interface Sci., 445 (2015) 303–311.

[8] H.M. Huang, J.H. Liu, L. Ding, Recovery of phosphate and ammonia nitrogen from the anaerobic digestion supernatant of activated sludge by chemical precipitation, J. Cleaner Prod., 102 (2015) 437–446.
[9] J. Das, B.S. Patra, N. Baliarsingh, K.M. Parida, Adsorption of phosphate by layered double hydroxides in aqueous solutions, Appl. Clay Sci., 32 (2006) 252–260.
[10] Z.G. Yuan, S. Pratt, D.J. Batstone, Phosphorus recovery from wastewater through microbial processes, Curr. Opin. Biotechnol., 23 (2012) 878–883.
[11] E.M. Van Voorthuizen, A. Zwijnenburg, M. Wessling, Nutrient removal by NF and RO membranes in a decentralized sanitation system, Water Res., 39 (2005) 3657–3667.
[12] T. Nur, M.A.H. Johir, P. Loganathan,S. Vigneswaran, J. Kandasamy, Effectiveness of purolite A500PS and A520E ion exchange resins on the removal of nitrate and phosphate from synthetic water, Desal. Water Treat., 47 (2012) 50–58.
[13] J. Vymazal, Removal of nutrients in various types of constructed wetlands, Sci. Total Environ., 380 (2007) 48–65.
[14] L.D. Hylander, A. Kietlińska, G. Renman, G. Simán, Phosphorus retention in filter materials for wastewater treatment and its subsequent suitability for plant production, Bioresour. Technol., 97 (2006) 914–921.
[15] Q.R. Zhang, J. Teng, G.D. Zou, Q.M. Peng, Q. Du, T.F. Jiao, J.Y. Xiang, Efficient phosphate sequestration for water purification by unique sandwich-like MXene/magnetic iron oxide nanocomposites, Nanoscale, 8 (2016) 7085–7093.
[16] C.G. Lee, J.A. Park, S.B. Kim, Phosphate removal from aqueous solutions using slag microspheres, Desal. Water Treat., 44 (2012) 229–236.
[17] H.Y. Shen, Z.J. Wang, A.M. Zhou, J.L. Chen, M.Q. Hu, X.Y. Dong, Q.H. Xia, Adsorption of phosphate onto aminefunctionalized nano-sized magnetic polymeradsorbents: mechanism and magnetic effects, RSC Adv., 28 (2015) 22080–22090.
[18] Y.G. Lai, W.J. Jiang, Z.S. Yang, X.P. Hao, R.Z. Xie, Equilibrium and kinetics studies of adsorption phosphate on raw and novel lithium silica fume based adsorbent, Desal. Water Treat., 57 (2016) 28794–28805.
[19] B.J. Pan, J. Wu, B.C. Pan, L. Lv, W.M. Zhang, L.L. Xiao, X.S. Wang, X.C. Tao, S.R. Zheng, Development of polymer-based nanosized hydrated ferric oxides (HFOs) for enhanced phosphate removal from waste effluents, Water Res., 43 (2009) 4421–4429.
[20] K.S. Triantafyllidis, E.N. Peleka, V.G. Komvokis, P.P. Mavros, Iron-modified hydrotalcite-like materials as highly efficient phosphate sorbents, J. Colloid Interface Sci., 342 (2010) 427–436.
[21] L. Chen, X. Zhao, B.C. Pan, W.X. Zhang, M. Hua, L. Lv, W.M. Zhang, Preferable removal of phosphate from water using hydrous zirconium oxide-based nanocomposite of high stability, J. Hazard. Mater., 284 (2015) 35–42.
[22] M. Mallet, K. Barthélémy, C. Ruby, A. Renard, S. Naille, Investigation of phosphate adsorption onto ferrihydrite by X-ray photoelectron spectroscopy, J. Colloid Interface Sci., 407 (2013) 95–101.
[23] E.A. Deliyanni, E.N. Peleka, N.K. Lazaridis, Comparative study of phosphates removal from aqueous solutions by nanocrystalline akaganéite and hybrid surfactant-akaganéite, Sep. Purif. Technol., 52 (2007) 478–486.
[24] R. Chitrakar, S. Tezuka, A. Sonoda, K. Sakane, K. Ooi, T. Hirotsu, Phosphate adsorption on synthetic goethite and akaganeite, J. Colloid Interface Sci., 298 (2006) 602–608.
[25] G.S. Zhang, H.J. Liu, R.P. Liu, J.H. Qu, Removal of phosphate from water by a Fe-Mn binary oxide adsorbent, J. Colloid Interface Sci., 335 (2009) 168–174.
[26] O.R. Harvey, R.D. Rhue, Kinetics and energetics of phosphate sorption in a multi-component Al(III)-Fe(III) hydr(oxide) sorbent system, J. Colloid Interface Sci., 322 (2008) 384–393.
[27] G.L. Li, S. Gao, G.S. Zhang, X.W. Zhang, Enhanced adsorption of phosphate from aqueous solution by nanostructured iron(III)-copper(II) binary oxides, Chem. Eng. J., 235 (2014) 124–131.
[28] Z.M. Ren, L.N. Shao, G.S. Zhang, Adsorption of phosphate from aqueous solution using an iron-zirconium binary oxide sorbent, Water Air Soil Pollut., 223 (2012) 4221–4231.
[29] J.B. Lu, D.F. Liu, J. Hao, G.W. Zhang, B. Lu, Phosphate removal from aqueous solutions by a nano-structured Fe-Ti bimetal oxide sorbent, Chem. Eng. Res. Des., 93 (2015) 652–661.
[30] Z. Marková, K.M. Šišková, J. Filip, J. Cˇuda, M. Kolář, K. Šafářová, I. Medřík, R. Zbořil, Air stable magnetic bimetallic Fe-Ag nanoparticles for advanced antimicrobial treatment and phosphorus removal, Environ. Sci. Technol., 47 (2013) 5285–5293.
[31] E. Saaremäe, M. Liira, M. Poolakese, T. Tamm, Removing phosphorus with Ca-Fe oxide granules-a possible wetlands filter material, Hydrol. Res., 45 (2014) 368–378.
[32] Y.Y. Zhang, B.C. Pan, C. Shan, X. Gao, Enhanced phosphate removal by nanosized hydrated La(III) oxide confined in cross-linked polystyrene networks, Environ. Sci. Technol., 50 (2016) 1447–1454.
[33] J.J. He, W. Wang, F.L. Sun, W.X. Shi, D.P. Qi, K. Wang, R.S. Shi, F.Y. Cui, C. Wang, X.D. Chen, Highly efficient phosphate scavenger based on well-dispersed $La(OH)_3$ nanorods in polyacrylonitrile nanofibers for nutrient-starvation antibacteria, ACS Nano, 9 (2015) 9292–9302.
[34] J. Xie, Y. Lin, C.J. Li, D.Y. Wu, H.N. Kong, Removal and recovery of phosphate from water by activated aluminum oxide and lanthanum oxide, Powder Technol., 269 (2015) 351–357.
[35] J. Xie, Z. Wang, S.Y. Lu, D.Y. Wu, Z.J. Zhang, H.N. Kong, Removal and recovery of phosphate from water by lanthanum hydroxide materials, Chem. Eng. J., 254 (2014) 163–170.
[36] L. Lai, Q. Xie, L.N. Chi, W. Gu, D.Y. Wu, Adsorption of phosphate from water by easily separable Fe_3O_4@SiO_2 core/shell magnetic nanoparticles functionalized with hydrous lanthanum oxide, J. Colloid Interface Sci., 465 (2016) 76–82.
[37] H. Qiu, C. Liang, J.H. Yu, Q.R. Zhang, M.X. Song, F.H. Chen, Preferable phosphate sequestration by nano-La(III) (hydr) oxides modified wheat straw with excellent properties in regeneration, Chem. Eng. J., 315 (2017) 345–354.
[38] V. Kuroki, G.E. Bosco, P.S. Fadini, A.A. Mozeto, A.R. Cestari, W.A. Carvalho, Use of a La(III)-modified bentonite for effective phosphate removal from aqueous media, J. Hazard. Mater., 274 (2014) 124–131.
[39] W.Y. Huang, Y. Zhu, J.P. Tang, X. Yu, X.L. Wang, D. Li, Y.M. Zhang, Lanthanum-doped ordered mesoporous hollow silica spheres as novel adsorbents for efficient phosphate removal, J. Mater. Chem., A 2 (2014) 8839–8848.
[40] L. Zhang, Q. Zhou, J.Y. Liu, N. Chang, L.H. Wan, J.H. Chen, Phosphate adsorption on lanthanum hydroxide-doped activated carbon fiber, Chem. Eng. J., 185 (2012) 160–167.
[41] H. Li, J.Y. Ru, W. Yin, X.H. Liu, J.Q. Wang, W.D. Zhang, Removal of phosphate from polluted water by lanthanum doped vesuvianite, J. Hazard. Mater., 168 (2009) 326–330.
[42] E.W. Shin, K.G. Karthikeyan, M.A. Tshabalala, Orthophosphate sorption onto lanthanum-treated lignocellulosic sorbents, Environ. Sci. Technol., 39 (2005) 6273–6279.
[43] W. Zhang, J. Fu, G.S. Zhang, X.W. Zhang, Enhanced arsenate removal by novel Fe-La composite (hydr)oxides synthesized via coprecipitation, Chem. Eng. J., 251 (2014) 69–79.
[44] P. Diffract, File, JCPDS International Centre Diffract, Data, PA 19073–3273 (2001).
[45] G.D. Wu, X.L. Wang, B. Chen, J.P. Li, N. Zhao, W. Wei, Y.H. Sun, Fluorine-modified mesoporous Mg-Al mixed oxides: mild and stable base catalysts for *O*-methylation of phenol with dimethyl carbonate, Appl. Catal., A 329 (2007) 106–111.
[46] S. Lagergren, About the theory of so-called adsorption of soluble substances, Handlingar, 24 (1898) 1–39.
[47] Y.S. Ho, G. McKay, Pseudo-second order model for sorption processes, Process Biochem., 34 (1999) 451–465.
[48] S.H. Chien, W.R. Clayton, Application of Elovich equation to the kinetics of phosphate release and sorption in soils, Soil Sci. Soc. Am. J., 44 (1980) 265–268.
[49] M. D'Arcy, D. Weiss, M. Bluck, R. Vilar, Adsorption kinetics, capacity and mechanism of arsenate and phosphate on a bifunctional TiO_2-Fe_2O_3 bi-composite, J. Colloid Interface Sci., 364 (2011) 205–212.

[50] W. Stumm, Chemistry of the solid-water interface: processes at the mineral-water and particle-water interface in natural systems, John Wiley & Sons, Inc., New York, 1992.
[51] M.B. McBride, A critique of diffuse double layer models applied to colloid and surface chemistry, Clays Clay Miner., 45 (1997) 598–608.
[52] F.H. Firsching, S.N. Brune, Solubility products of the trivalent rare-earth phosphates, J. Chem. Eng. Data, 36 (1991) 93–95.
[53] I. Langmuir, The constitution and fundamental properties of solids and liquids. Part I. Solids, J. Am. Chem. Soc., 38 (1916) 2221–2295.
[54] H. Freundlich, Über die adsorption in lösungen, Z. Phys. Chem., 57 (1906) 385–470.
[55] L. Zeng, X.M. Li, J.D. Liu, Adsorptive removal of phosphate from aqueous solutions using iron oxide tailings, Water Res., 38 (2004) 1318–1326.
[56] H.L. Liu, X.F. Sun, C.Q. Yin, C. Hu, Removal of phosphate by mesoporous ZrO_2, J. Hazard. Mater., 151 (2008) 616–622.
[57] Q.M. Peng, J.X. Guo, Q.R. Zhang, J.Y. Xiang, B.Z. Liu, A.G. Zhou, R.P. Liu, Y.J. Tian, Unique lead adsorption behavior of activated hydroxyl group in two-dimensional titanium carbide, J. Am. Chem. Soc., 136 (2014) 4113–4116.
[58] S.Y. Bao, L.H. Tang, K. Li, P. Ning, J.H. Peng, H.B. Guo, T.T. Zhu, Y. Liu, Highly selective removal of Zn(II) ion from hot-dip galvanizing pickling waste with amino-functionalized Fe_3O_4@SiO_2 magnetic nano-adsorbent, J. Colloid Interface Sci., 462 (2016) 235–242.
[59] Q.R. Zhang,Q. Du,M. Hua, T.F. Jiao, F.M. Gao, B.C. Pan, Sorption enhancement of lead Ions from water by surface charged polystyrene-supported nano-zirconium oxide composites, Environ. Sci. Technol., 47 (2013) 6536–6544.
[60] W. Stumm, J.J. Morgan, Aquatic chemistry: chemical equilibria and rates in natural waters, John Wiley & Sons, Inc., New York, 2012.
[61] S. Goldberg, C.T. Johnston, Mechanisms of arsenic adsorption on amorphous oxides evaluated using macroscopic measurements, vibrational spectroscopy, and surface complexation modeling, J. Colloid Interface Sci., 234 (2001) 204–216.
[62] X.X. Fan, T. Yu, Y. Wang, J. Zheng, L. Gao, Z.S. Li, J.H. Ye, Z.G. Zou, Role of phosphorus in synthesis of phosphated mesoporous TiO_2 photocatalytic materials by EISA method, Appl. Surf. Sci., 254 (2008) 5191–5198.
[63] M. Textor, L. Ruiz, R. Hofer, A. Rossi, K. Feldman, G. Hähner, N.D. Spencer, Structural chemistry of self-assembled monolayers of octadecylphosphoric acid on tantalum oxide surfaces, Langmuir, 16 (2000) 3257–3271.
[64] E. Kobayashi, M. Ando, Y. Tsutsumi, H. Doi, T. Yoneyama, M. Kobayashi, T. Hanawa, Inhibition effect of zirconium coating on calcium phosphate precipitation of titanium to avoid assimilation with bone, Mater. Trans., 48 (2007) 301–306.
[65] J.F. Moulder, J. Chastain, R.C. King, Handbook of X-ray photoelectron spectroscopy: a reference book of standard spectra for identification and interpretation of XPS data, Eden Prairie, MN: Perkin-Elmer, 1992.
[66] D.S. Soejoko, M.O. Tjia, Infrared spectroscopy and X ray diffraction study on the morphological variations of carbonate and phosphate compounds in giant prawn (Macrobrachium rosenbergii) skeletons during its moulting period, J. Mater. Sci., 38 (2003) 2087–2093.

Supplementary materials

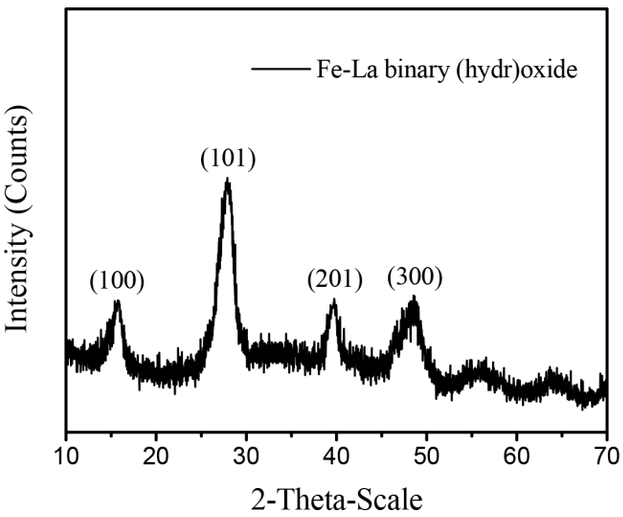

Fig. S1. XRD patterns of the Fe-La binary (hydro) oxide.

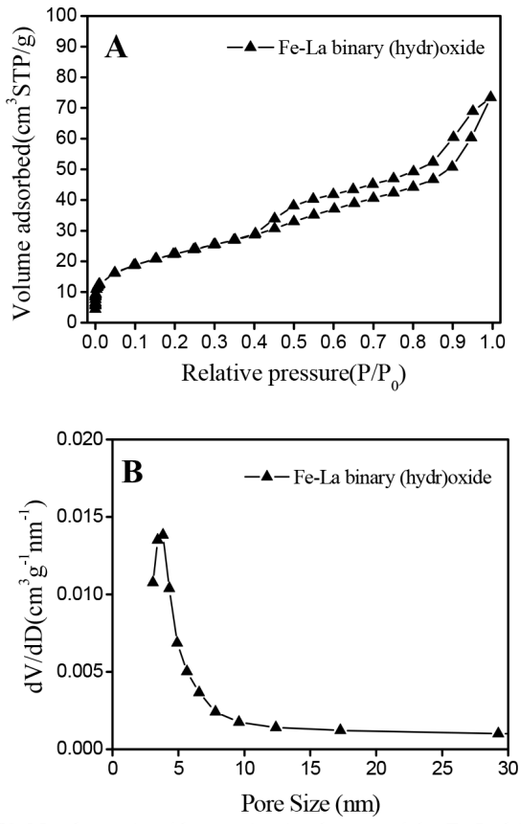

Fig. S2. N_2 adsorption/desorption isotherms of the Fe-La binary (hydro) oxide (A) and Pore differential distribution of the Fe-La binary (hydro)oxide (B).

Table S1
BET specific surface area and porosity measurements of the Fe-La binary (hydro)oxide

Adsorbent	Fe-La
Specific surface area (m^2/g)	120.1
Average pore diameter (Å)	56.0
Average pore volume (cm^3/g)	0.168

Table S2
O1s peak parameters for the Fe-La binary (hydro) oxide before and after phosphate adsorption

Sample	Peak	B. E. (eV)	Percent (%)
Fe-La	O_2^-	530.02	13.4
	OH^-	531.13	40.9
	H_2O	531.98	45.7
Fe-La-P	O_2^-	530.1	45.9
	OH^-	531.01	27.2
	H_2O	532	26.9